LASER INTERFEROMETER GRAVITATIONAL WAVE OBSERVATORY
- LIGO -
CALIFORNIA INSTITUTE OF TECHNOLOGY
MASSACHUSETTS INSTITUTE OF TECHNOLOGY

Technical Note	**LIGO-T1200450-v1**	2012/09/25

Cavity alignment fluctuations in the H2 One Arm Test

L. Barsotti for the ISC

California Institute of Technology
LIGO Project, MS 100-36
Pasadena, CA 91125
Phone (626) 395-2129
Fax (626) 304-9834
E-mail: info@ligo.caltech.edu

Massachusetts Institute of Technology
LIGO Project, Room NW17-161
Cambridge, MA 02139
Phone (617) 253-4824
Fax (617) 253-7014
E-mail: info@ligo.mit.edu

LIGO Hanford Observatory
Route 10, Mile Marker 2
Richland, WA 99352
Phone (509) 372-8106
Fax (509) 372-8137
E-mail: info@ligo.caltech.edu

LIGO Livingston Observatory
19100 LIGO Lane
Livingston, LA 70754
Phone (225) 686-3100
Fax (225) 686-7189
E-mail: info@ligo.caltech.edu

WWW: http://www.ligo.caltech.edu/

Abstract

The PITCH and YAW angular motion of the test masses in the H2 OAT was measured to be less than 0.1 μrad rms, without any angular control feedback applied. The angular motion was sufficiently low that it did not limit the cavity stability, showing that an active angular control is not needed in aLIGO to operate the arm cavities. A drift control was anyway tested by using the WFSs in reflection to the cavity, but a strong PITCH to YAW coupling in the WFS set-up prevented us from seeing any benefit.

1 Introduction

Two different types of sensors have been used to measure the angular fluctuations of the H2 One Arm cavity: optical levers, sensing the angular motion of the test masses relative to ground, and a pair of RF Wave Front Sensors (WFSs), looking at the beam reflected by the cavity.

The data analyzed in this note are the following:

- **Data Set 1**: GPS 1031000346-846: the cavity was locked, the angular loops were open. The ISI configuration is summarized in vincent.lhuillier entry 4136. These data have been used to analyze the angular motion as measured by the optical levers and the WFSs, and to compare the angular motion of the test masses against the expected motion given the input seismic noise (as measured by the ISI) and the model of the QUAD suspension;
- **Data Set 2**: September 7, 2012 starting @ 3:00:00 UTC keita.kawabe entry 4126. These data correspond to the time in which the WFS and optical lever sensing matrices have been measured.
- **Data Set 3**: ON/OFF comparison of the angular control loops (September 7, 2012 3:50:00 UTC - OFF, September 7, 2012 3:50:00 UTC - ON).

2 Optical Lever Signals

Figures 1 and 2 show the ETMY and ITMY optical lever spectra for PITCH and YAW (calibrated as explained in jeffrey.kissel entry 3773).

Note that the EY optical lever setup has a very length to angle coupling (see appendix A, so that the signal below 100 mHz is not the actual motion of the test mass.

There is a factor 2 difference between ETMY and ITMY in the amplitude of the two main peaks between 400 - 600 mHz in PITCH. This is due to a difference in the input seismic noise as measured by the ISI, and it is currently under investigation.

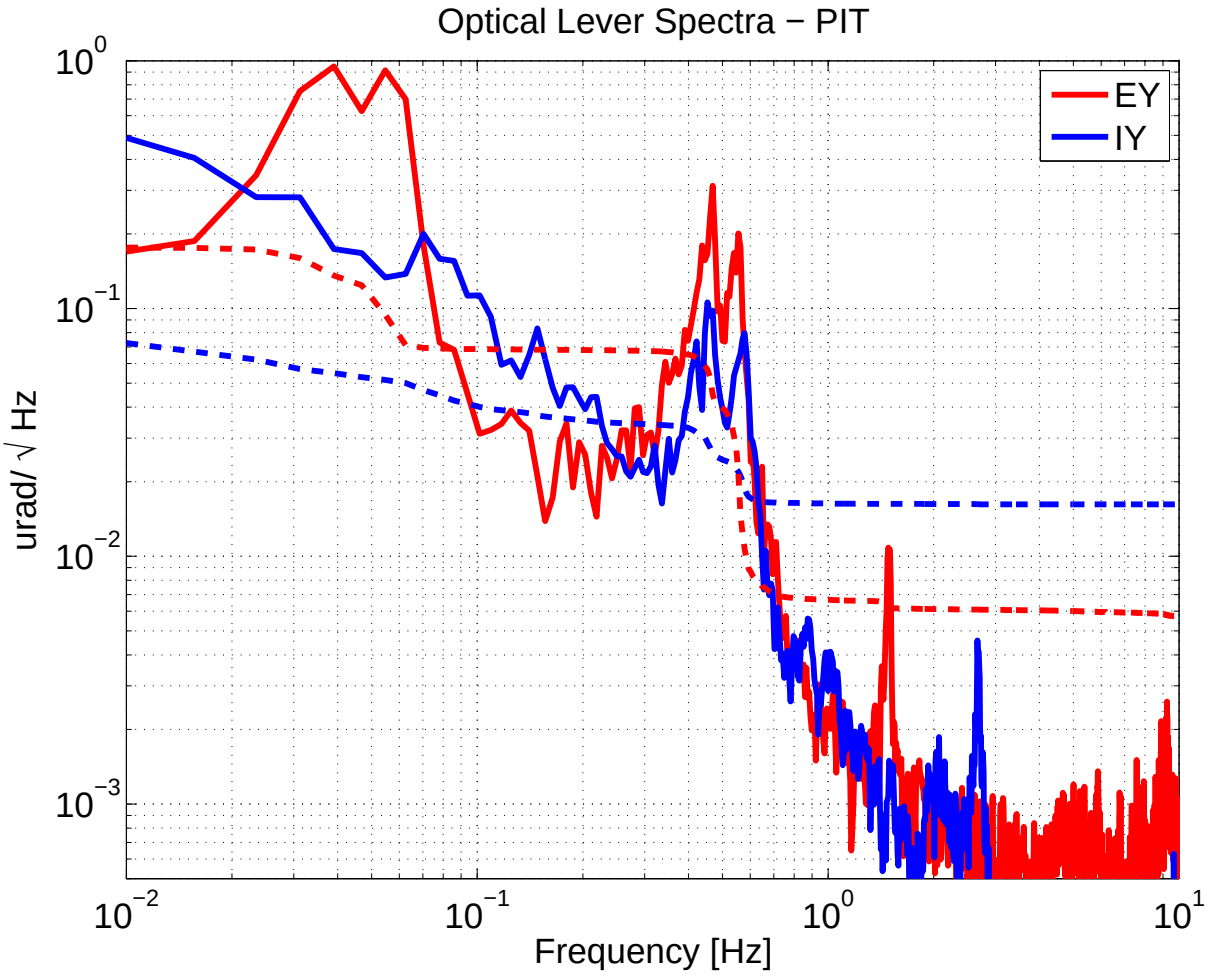

Figure 1: Spectra of the optical Lever signals for PITCH - ASC loops open. The EY spectrum is dominated by the length to pitch coupling in the optical lever itself.

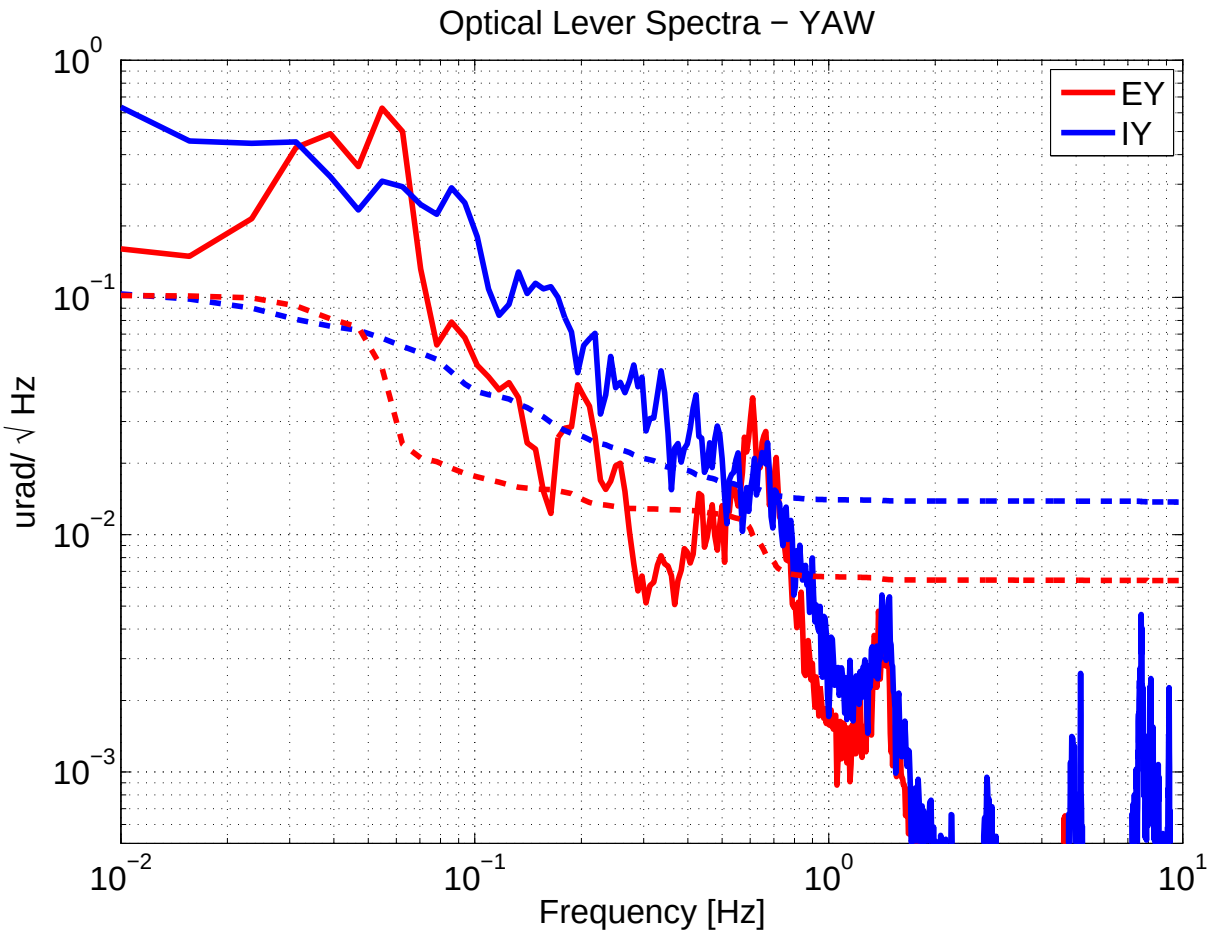

Figure 2: Spectra of the optical lever signals for YAW- ASC loops open. As for PITCH, the EY spectrum is dominated by the length to angle coupling in the optical lever itself.

3 Calibration of WFS signals

The spectra of the WFS signals are shown in figure 3.

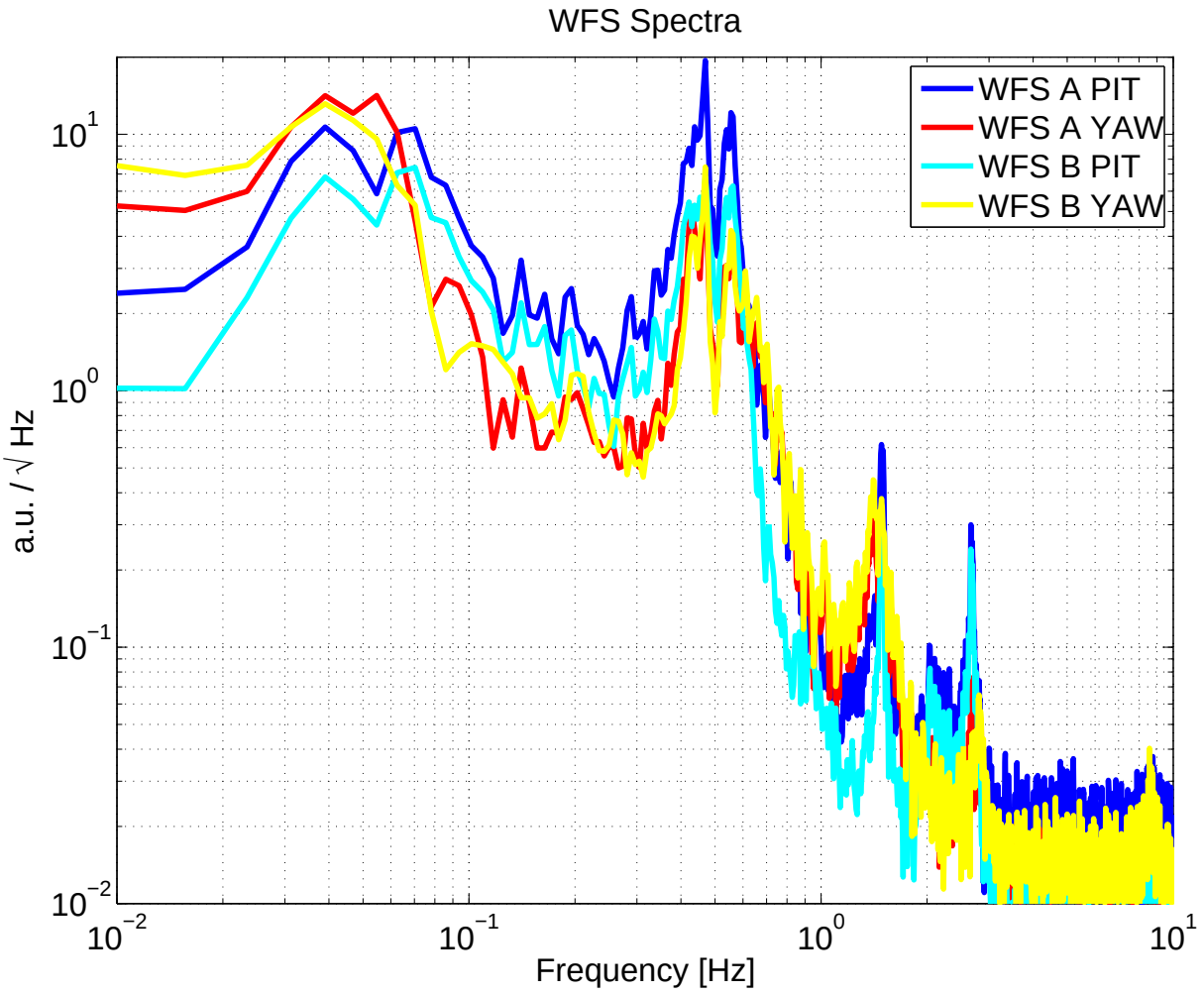

Figure 3: WFS spectra.

The WFS signals have been calibrated by using the optical lever signals (data set 2). Here are the matrices in μrad of test mass angular motion per counts of the WFS signals:

$$\begin{pmatrix} Angle\_EY\_PIT[\mu rad] \\ Angle\_IY\_PIT[\mu rad] \end{pmatrix} = \begin{pmatrix} 0.0556 & -0.0680 \\ -0.0306 & 0.0601 \end{pmatrix} \begin{pmatrix} WFS\_A\_PIT[ct] \\ WFS\_B\_PIT[ct] \end{pmatrix} \quad (3.1)$$

$$\begin{pmatrix} Angle\_EY\_YAW[\mu rad] \\ Angle\_IY\_YAW[\mu rad] \end{pmatrix} = \begin{pmatrix} 0.0953 & -0.0608 \\ 0.0596 & -0.0508 \end{pmatrix} \begin{pmatrix} WFS\_A\_PIT[ct] \\ WFS\_B\_PIT[ct] \end{pmatrix} \quad (3.2)$$

The mirror motion as measured by the WFSs is shown in figures 4 5, compared with the optical lever signals.

For PITCH, the agreement is very good. For ETMY, the discrepancy at low frequency is due to the fact the optical lever has a large length to pitch coupling, so the ETMY optical lever overestimate the PITCH angular motion RMS by a factor 2.

For YAW, the angular motion predicted by the WFSs is wrong, as PITCH to YAW coupling in the WFS set-up is very large. The EY spectrum based on the optical lever is again dominated by the length to yaw coupling of the optical lever itself.

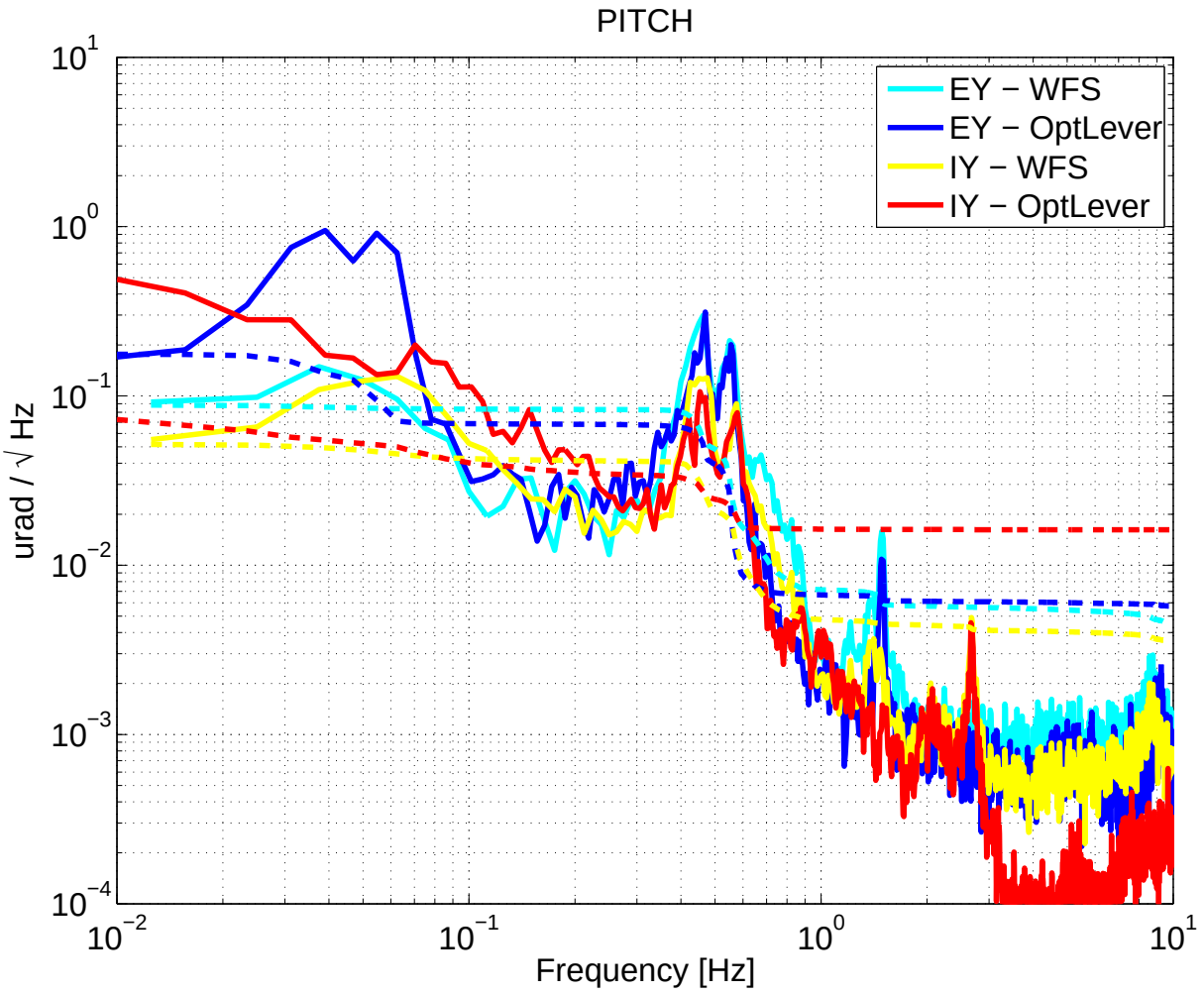

Figure 4: Calibrated WFS signals, compared to the optical lever spectra - PITCH

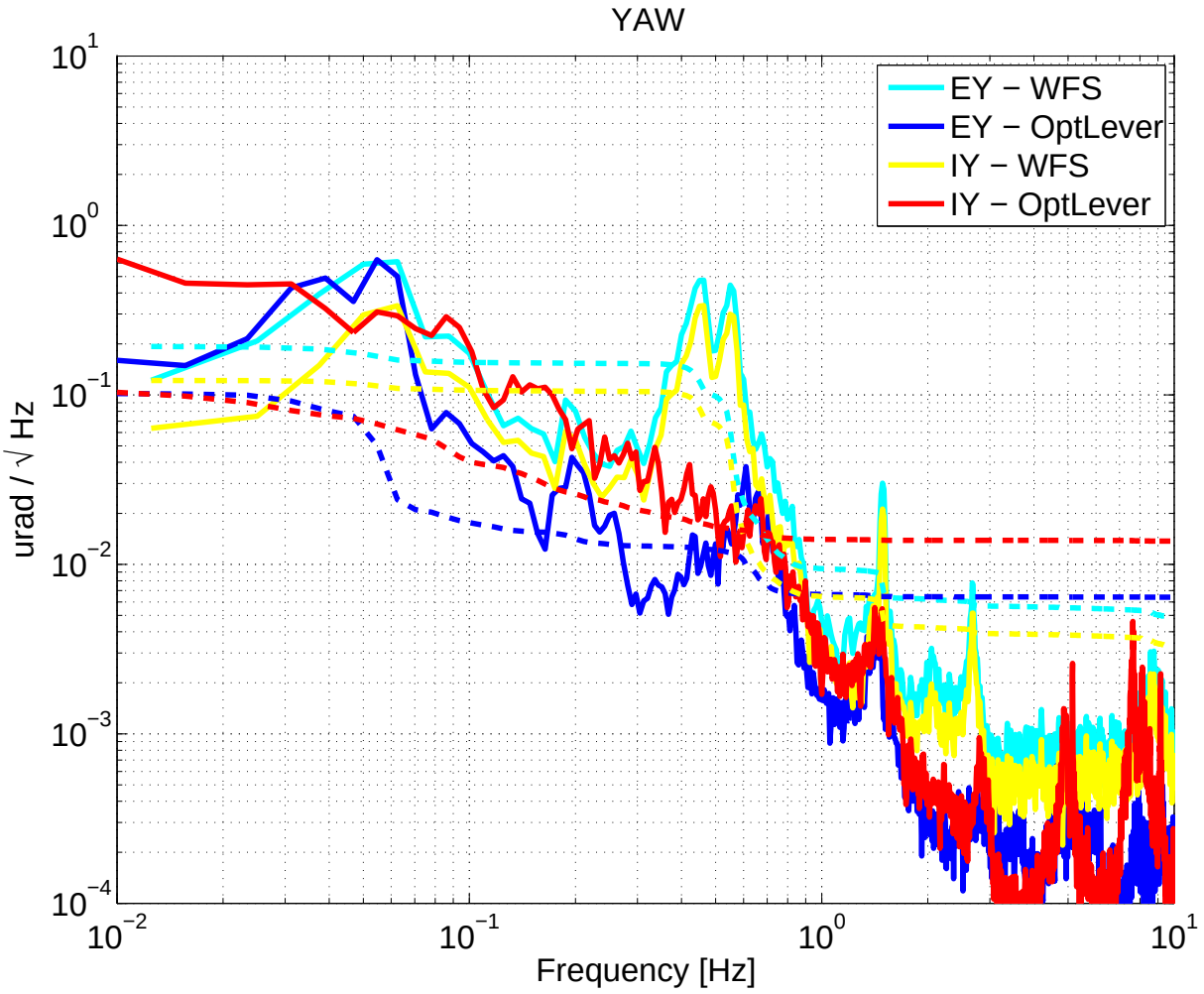

Figure 5: Calibrated WFS signals, compared to the optical lever spectra - YAW

3.1 WFS PITCH/YAW Cross-coupling

One example of the large PITCH to YAW coupling in the WFS signals is shown in figure 6: when the PITCH common degree of freedom is excited (ANG_PIT, in pink) a response is visible not only in WFS_PIT, but also in WFS_YAW, and it is only a factor 2 smaller than what you get in WFS_YAW for an actual YAW excitation.

The fact that WFS_YAW is dominated by PITCH is also evident just by looking at the WFS_YAW spectra 3, which show the same typical PITCH structures between 400-600 mHz, which are not present in the optical lever YAW spectra.

The reason for this large cross coupling has not been investigated due to time constraints. However, it seems to be related to a specific problem of this WFS set-up. As the OAT showed that an angular control is not needed for operating the cavity, and therefore it won't be implemented in aLIGO, no further analysis will be performed.

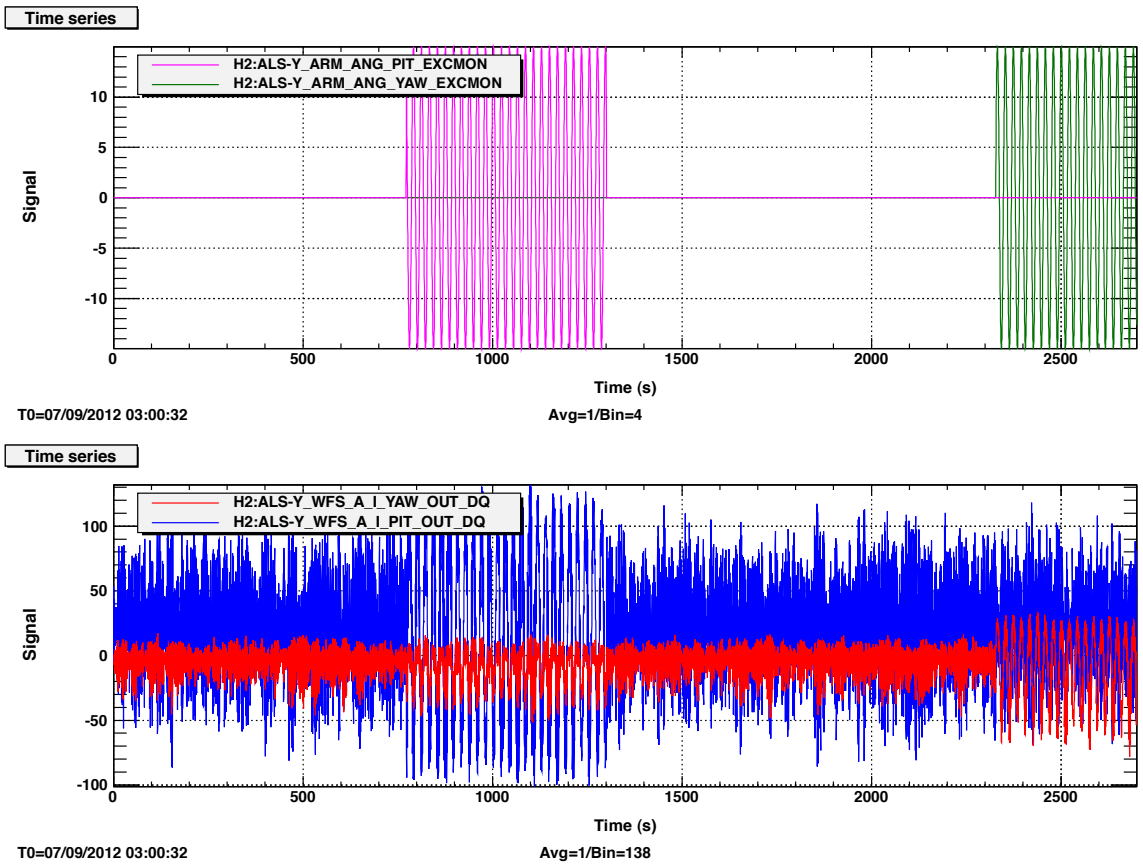

Figure 6: Excitation in ANG (PIT purple, YAW green).

4 Drift control ON/OFF

The performance of the drift control tested during the OAT is shown in figures 7 8. The drift control was implemented by feeding-back the WFS signals to the PUM stage of the QUAD. It is evident from the plots that the error signals were reduced in the loop bandwidth as expected (bottom plots), but the big coupling between PITCH and YAW caused the YAW angular motion of the test masses to increase significantly. The drift control was reintroducing some noise in PITCH as well.

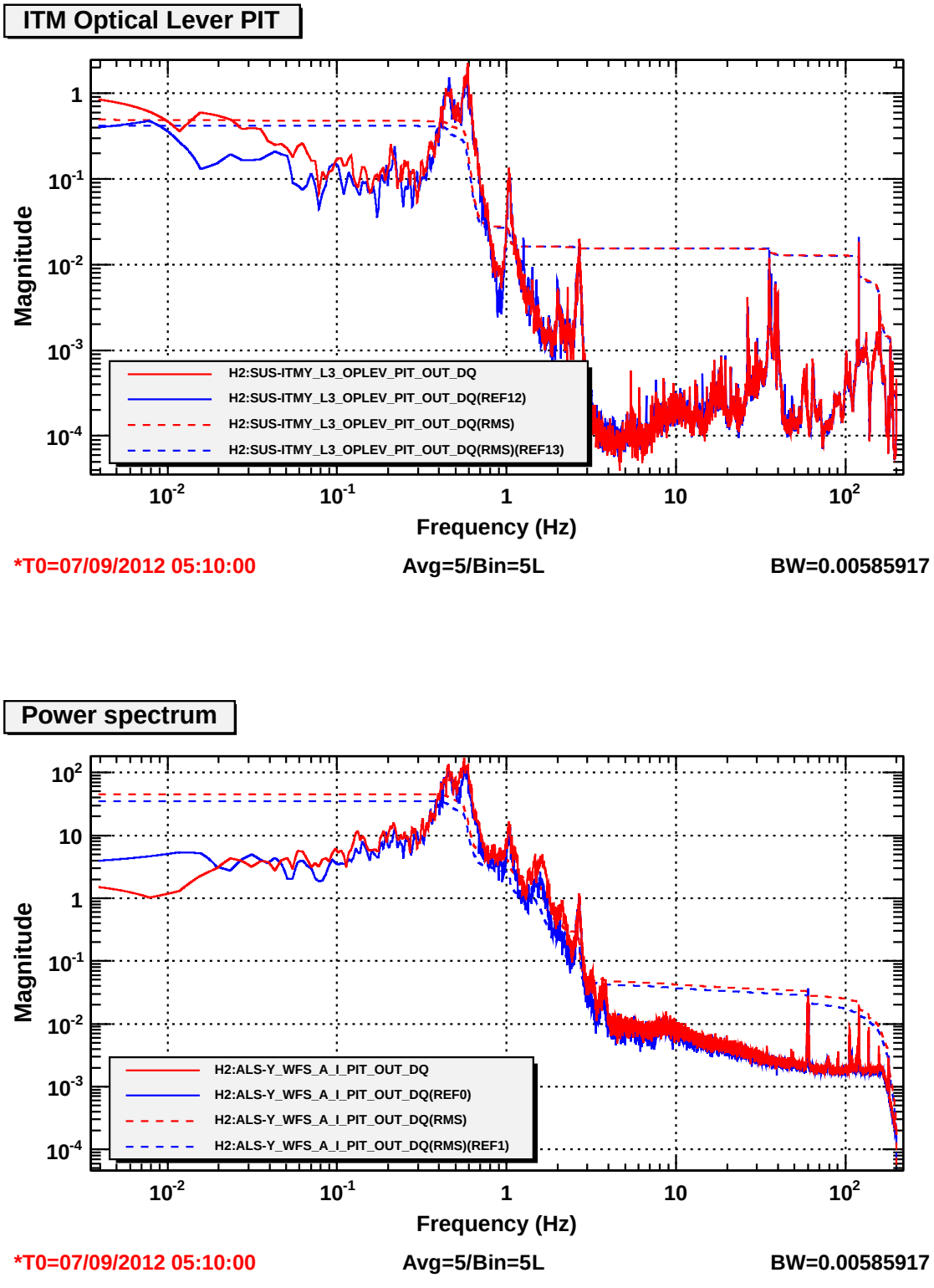

Figure 7: PITCH spectra of optical levers (TOP) and WFSs (BOTTOM) - RED: ASC loops ON, BLUE: ASC loops OFF

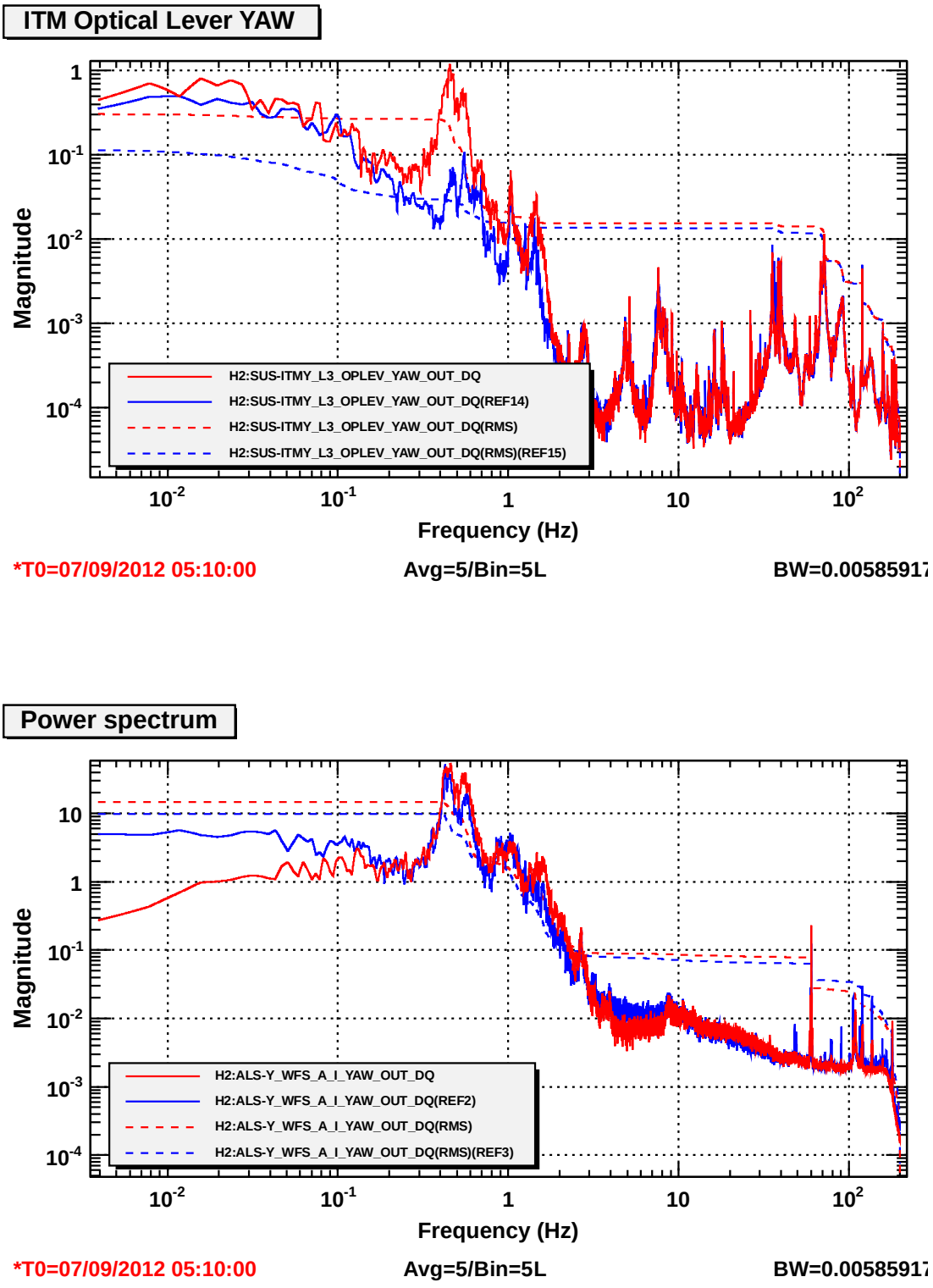

Figure 8: YAW spectra of optical levers (TOP) and WFSs (BOTTOM) - RED: ASC loops ON, BLUE: ASC loops OFF

5 Conclusions

The angular motion of the QUAD test masses have been measured to be less than 0.1 μrad RMS without any angular feed-back implemented, and it is compatible with reliable operation of the arm cavity.

A Length to angle coupling in Optical Levers

Low frequency part of optical lever signals dominated by Length2Angle coupling in the optical levers E1200836-v1

Table 1: default

	PIT $[mrad/m]$	YAW $[mrad/m]$
ITM-Y	0.76	0.4
ETM-Y	61.36	32.6

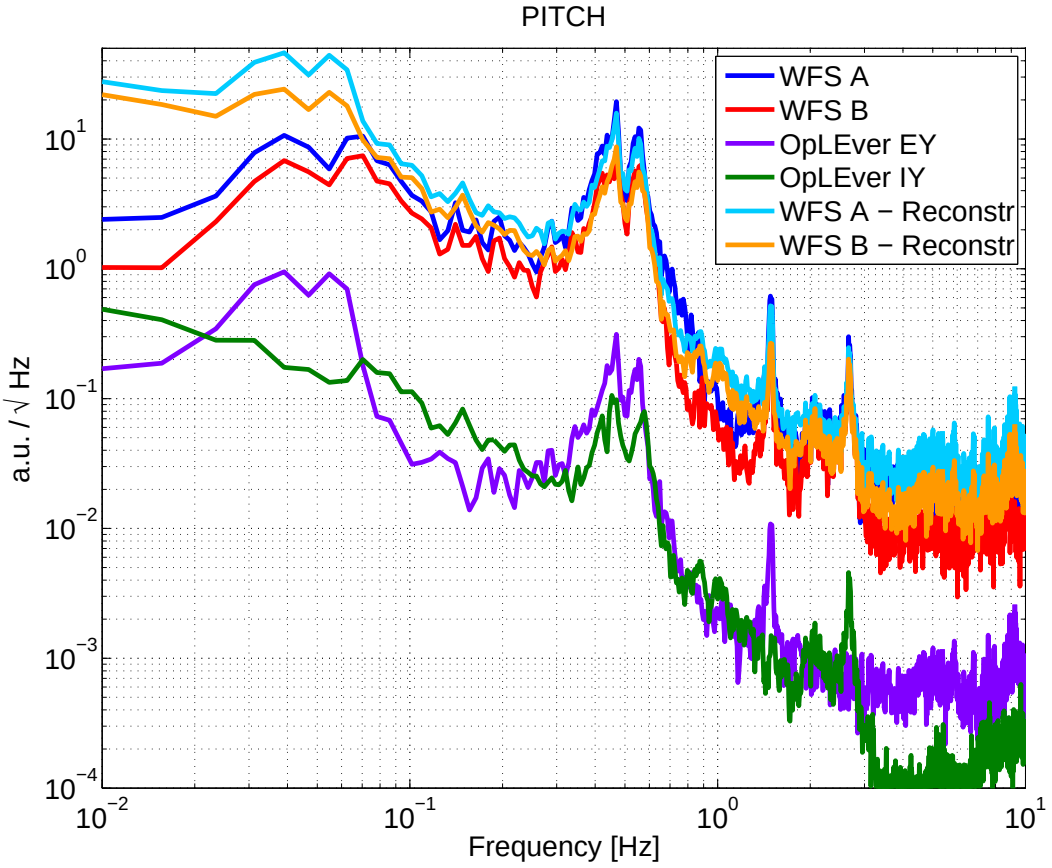

Figure 9: WFS signals reconstructed from optical lever signals. The mismatch at low frequency is due to the fact that there is a length to angle coupling due to the optical lever set-up.

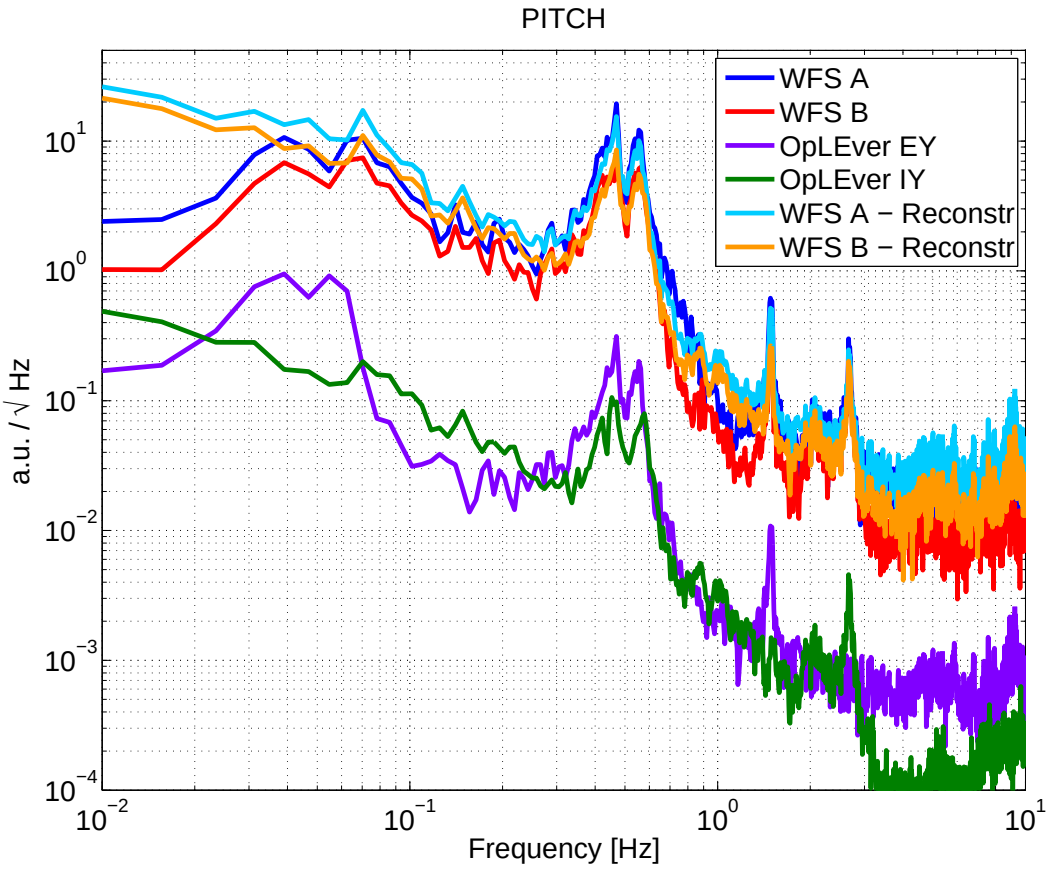

Figure 10: WFS signals reconstructed from Optical Lever signals with subtraction of optical lever length (as measured by the calibrated longitudinal arm motion) to pitch.

B WFS and optical lever calibration matrices

ANG and POS correspond to the common and differential angular degrees of freedom of the cavity. The transfer matrices from ANG / POS to WFS and Optical lever signals are:

$$\begin{pmatrix} WFS\_A\_PIT[au] \\ WFS\_B\_PIT[au] \end{pmatrix} = \begin{pmatrix} 0.047 & -5.66 \\ 0.906 & -3.76 \end{pmatrix} \begin{pmatrix} POS[au] \\ ANG[au] \end{pmatrix} \tag{B.1}$$

$$\begin{pmatrix} Angle\_EY\_PIT[\mu rad] \\ Angle\_IY\_PIT[\mu rad] \end{pmatrix} = \begin{pmatrix} -0.059 & -0.059 \\ -0.053 & 0.053 \end{pmatrix} \begin{pmatrix} POS[au] \\ ANG[au] \end{pmatrix} \tag{B.2}$$

$$\begin{pmatrix} WFS\_A\_YAW[au] \\ WFS\_B\_YAW[au] \end{pmatrix} = \begin{pmatrix} 0.086 & 2.379 \\ -0.293 & 3.302 \end{pmatrix} \begin{pmatrix} POS[au] \\ ANG[au] \end{pmatrix} \tag{B.3}$$

$$\begin{pmatrix} Angle\_EY\_YAW[\mu rad] \\ Angle\_IY\_YAW[\mu rad] \end{pmatrix} = \begin{pmatrix} 0.026 & 0.026 \\ -0.026 & 0.026 \end{pmatrix} \begin{pmatrix} POS[au] \\ ANG[au] \end{pmatrix} \tag{B.4}$$